

Controlled large strain of Ni silicide/Si/Ni silicide nanowire heterostructures and their electron transport properties

W. W. Wu, K. C. Lu, K. N. Chen, P. H. Yeh, C. W. Wang, Y. C. Lin, and Yu Huang

Citation: *Applied Physics Letters* **97**, 203110 (2010); doi: 10.1063/1.3515421

View online: <http://dx.doi.org/10.1063/1.3515421>

View Table of Contents: <http://scitation.aip.org/content/aip/journal/apl/97/20?ver=pdfcov>

Published by the [AIP Publishing](#)

Articles you may be interested in

[Large piezoresistance of single silicon nano-needles induced by non-uniaxial strain](#)

J. Appl. Phys. **110**, 114323 (2011); 10.1063/1.3662917

[Advanced core/multishell germanium/silicon nanowire heterostructures: Morphology and transport](#)

Appl. Phys. Lett. **98**, 163112 (2011); 10.1063/1.3574537

[Tunnel field-effect transistor using InAs nanowire/Si heterojunction](#)

Appl. Phys. Lett. **98**, 083114 (2011); 10.1063/1.3558729

[Controllable deformation of silicon nanowires with strain up to 24%](#)

J. Appl. Phys. **107**, 124314 (2010); 10.1063/1.3436589

[Band engineered epitaxial Ge – Si_xGe_{1-x} core-shell nanowire heterostructures](#)

Appl. Phys. Lett. **95**, 033101 (2009); 10.1063/1.3173811

The advertisement features a dark blue background with a subtle grid pattern. At the top left, the text 'NEW! Asylum Research MFP-3D Infinity™ AFM' is written in white and orange, followed by 'Unmatched Performance, Versatility and Support' in orange. The Oxford Instruments logo, consisting of the word 'OXFORD' above 'INSTRUMENTS' in a white box, is positioned at the top right, with the tagline 'The Business of Science®' below it. The central part of the ad is divided into four quadrants by diagonal lines. The top-left quadrant shows a blue and white AFM image with the text 'Stunning high performance'. The top-right quadrant shows a brown and white AFM image with the text 'Simpler than ever to GetStarted™'. The bottom-left quadrant shows a yellow and white AFM image with the text 'Comprehensive tools for nanomechanics'. The bottom-right quadrant shows a yellow and white AFM image with the text 'Widest range of accessories for materials science and bioscience'. On the right side, there is a photograph of the MFP-3D Infinity AFM system, including the main unit and a smaller probe head.

Controlled large strain of Ni silicide/Si/Ni silicide nanowire heterostructures and their electron transport properties

W. W. Wu,^{1,a)} K. C. Lu,^{2,a)} K. N. Chen,^{3,a)} P. H. Yeh,⁴ C. W. Wang,¹ Y. C. Lin,⁵ and Yu Huang⁵

¹Department of Materials Science and Engineering, National Chiao Tung University, Hsinchu 300, Taiwan

²Department of Materials Science and Engineering, National Cheng Kung University, Tainan 701, Taiwan

³Department of Electronics Engineering, National Chiao Tung University, Hsinchu 300, Taiwan

⁴Department of Physics, Tam Kang University, Taipei 251, Taiwan

⁵Department of Materials Science and Engineering, University of California, Los Angeles, Los Angeles, California 90095-1595, USA

(Received 4 September 2010; accepted 22 October 2010; published online 18 November 2010)

Unusually large and compressively strained Si in nanoheterostructures of Ni silicide/Si/Ni silicide, in which the strain of the Si region can be achieved up to 10%, has been produced with point contact reactions between Si and Ni nanowires in an ultrahigh vacuum transmission electron microscope. The growth rate and relationships between the strain and the spacing of the Si region have been measured. Based on the rate and relationships, we can control the Si dimension and, in turn, the strain of remaining Si can be tuned with appropriate spacing. Since one-dimensional nanoheterostructures may have potential applications in nanoelectronic devices, the existent strain will further affect carrier mobility and piezoresistance coefficients in the Si region. Electrical measurements on the nanodevices from such nanoheterostructures show that the current output closely correlates with the Si channel length and compressive strain. © 2010 American Institute of Physics. [doi:10.1063/1.3515421]

Semiconductor nanowires are attractive components for future nanoelectronics since they can exhibit a range of device functions and serve as bridging wires that connect to larger scale metallization.¹⁻⁵ Recently, heterostructure formation in one-dimensional nanostructures (nanowires) is equally important for their potential applications as efficient light emitting sources and field effect transistor.⁶⁻⁸

For strain engineering, it is now considered to be one of the most promising strategies for developing high-performance sub-10-nm silicon devices.⁹ Furthermore, strained Si technology has become the leading approach to further improve the metal-oxide-semiconductor field effect transistor performance as the continuous device scaling faces its physical limitation.¹⁰⁻¹² By introducing strain in the Si channel region, the carrier mobility is enhanced, and the transistor drive current is improved.¹²

To realize this potential, we fabricate NiSi/Si/NiSi nanowire heterostructures utilizing *in situ* point contact reactions between Ni and Si nanowires in a high-resolution transmission electron microscope (TEM). *In situ* TEM is a powerful technique which is well suited to answer many questions about nanostructures.¹³⁻²² In this paper, we report that the giant existent strain in the remaining Si of NiSi/Si/NiSi nanowire heterostructure was observed. By choosing appropriate imaging conditions, the remaining length of the Si region can be controlled with atomically flat NiSi/Si interfaces.²¹

Silicon nanowires were prepared on a p-type Si wafer by the vapor-liquid-solid method using nano-Au dots as nucleation sites. The resultant single-crystal Si nanowires are

along a [111] growth direction²³⁻²⁵ and with thin surface oxide (~1–5 nm thick). Polycrystalline Ni nanowires were synthesized via the anodic aluminum oxidation method and stored in isopropanol.²⁶ The Ni nanowires and Si nanowires with lengths of a few microns ranged in diameter from 10 to 40 nm.

To prepare point contact samples, we put droplets of both solutions on Si grids with a square opening covered with a window of a glassy Si₃N₄ film. The thickness of the Si₃N₄ film is about 20 nm so that it is transparent to the electron beam and does not interfere with the imaging of the nanowires. The samples were dried under light bulbs. TEM examinations were conducted in a Japan Electron Optics Laboratory (JEOL) 2000 V ultrahigh vacuum TEM (UHV-TEM) under a base pressure of 3×10^{-10} Torr, where a sample can be heated to 1000 °C. Upon heating in UHV-TEM, Ni atoms would diffuse into Si nanowires to form NiSi nanowires. Phase identification was carried out by diffraction pattern and energy dispersion x-ray spectrometer (EDS) analysis.

From the point contact reaction, Ni atoms dissolve and diffuse interstitially in Si (Ref. 27) and stop at the ends of the Si nanowire, thereby nucleating the growth of Ni silicide to form a Ni silicide nanowire.^{21,22} Figure 1 shows a TEM image of the formation of nickel silicide from both ends of a Si nanowire at 700 °C annealing. If annealing is stopped before the entire nanowire transforms into NiSi, a Ni silicide/Si/Ni silicide nanoheterostructure is formed. From high-resolution TEM images, selected area diffraction patterns, and EDS analysis, we identified the structure of the silicide to be single-crystal NiSi.^{21,22} The darker regions at the two ends are NiSi and the lighter region in the middle is Si. Notably, since the annealing temperature was 700 °C and volatile materials existed in the sample, the vacuum would be degraded

^{a)} Authors to whom correspondence should be addressed. Electronic addresses: wwwu@mail.nctu.edu.tw, gkclu@mail.ncku.edu.tw, and knchen@mail.nctu.edu.tw.

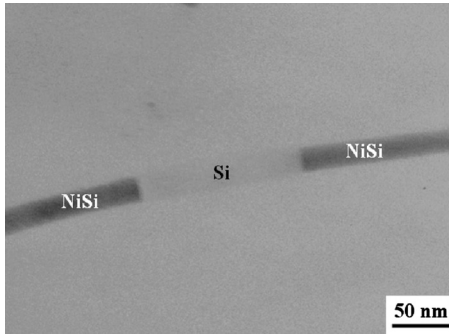


FIG. 1. TEM image of the NiSi/Si/NiSi heterostructure. The bright area is Si and the dark area is NiSi.

to 10^{-8} Torr as the annealing occurred; under such conditions, the surface oxide surrounding the Si was still stable enough to confine the diameter of the silicide grains.

Figures 2(a)–2(c) show a set of high-resolution TEM images of the atomically flat NiSi/Si interface taken as the interface advances into the Si. The interface is parallel to the (111) plane of Si. From the high-resolution TEM images, we can measure the dimension of the Si region, count the number of the Si atomic layers inside, and then calculate the average interplanar spacing. As a consequence, it was found that the average interplanar spacing decreased as the two NiSi/Si interfaces moved closer. The remaining Si with average lattice spacing of 0.301, 0.296, and 0.292 nm is shown, respectively. There is already compressive strain of 7% in comparison with the original lattice spacing.

Figure 3 shows the relationship between the compressive strain compared with the average interplanar spacing of Si (111) without annealing and the spacing of the Si region in the NiSi/Si/NiSi nanoheterostructure. It is surprising that the remaining Si exhibited unusually large and compressive strain which increased as the dimension of the remaining Si decreased. On the basis of the results from Figs. 2 and 3, it

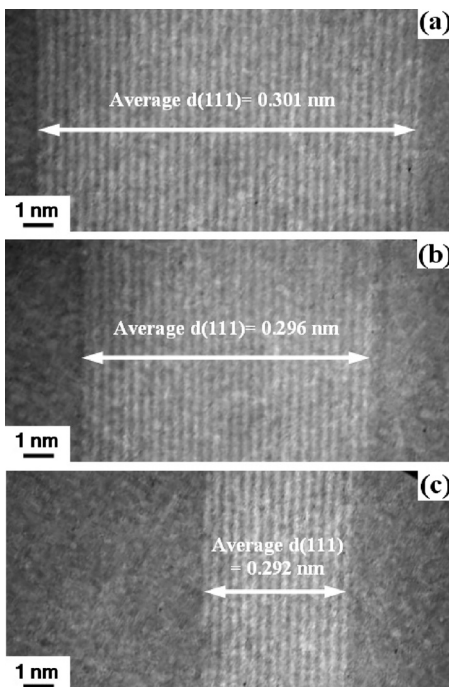


FIG. 2. *In situ* high-resolution TEM image sequence of the growth of NiSi/Si/NiSi heterostructures. The bright and dark portions of the lattice images correspond to Si and NiSi, respectively.

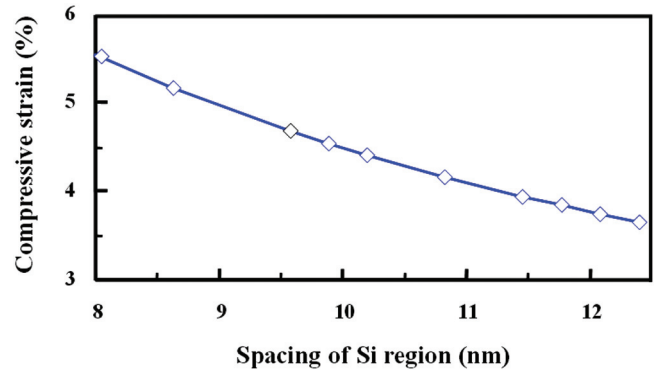


FIG. 3. (Color) Plot of the compressive strain vs the spacing of Si region in the nanoheterostructure NiSi/Si/NiSi.

can be inferred that as the dimension continues to shrink, the compressive strain of the Si region would be up to 10%. According to previous studies, as the remaining Si dimension is down to less than 2 nm, the lattice strain can be up to 12%.²¹

In the process of NiSi formation, the diffusion of Ni atoms into Si lattice could have led to volume expansion. However, due to the difference in the interplanar spacing of Si and NiSi across the epitaxial interface, Si would be stretched radially at the interface. Thus, on the basis of Poisson's ratio,²⁸ Si will be compressed axially. On the other hand, for fixed strain energy, the average energy distributed per atomic layer in the Si would be larger in a smaller Si region; as a consequence, the strain increased when the dimension of the Si region decreased.

It is well known that Ni is the dominant diffusion species in the interfacial reactions between Ni and Si,²⁹ which leads to the fact that Ni atoms diffuse into the Si lattice and tend to separate Si atoms a little bit. As the distance among Si atoms is extended, the diameter of a nanowire will be extended. We can calculate it theoretically based on the crystal structures of Si and NiSi. As we know the crystal structures, lattice constants, and the number of Si atoms per unit cell, the volume occupied by per Si atom can be obtained.

The strain of the heterostructures is mainly attributed to the mismatch between the two lattices; also, as the thickness reaches critical thickness, there would be dislocations generated, contributing to strain relaxation. Therefore, most of the strains are within 10%.³⁰

In our previous studies, we have investigated the interfaces of the heterostructures by high-resolution TEM, finding that there is no generation of dislocations at the interface. The main reason is that it is very difficult for dislocations to nucleate at such diameter.³¹ Additionally, the existence of the epitaxial growth at the interface lowers the chances of dislocation generation. Thus, without dislocation relaxation, compressive strain increases as the remaining Si region decreases.

As for the amount of strain, based on previous studies, lattice mismatch of 5.6% exists at the NiSi/Si interface. Since volume strain is about three times of linear strain, there is about 17% change in the volume of NiSi as Si is converted to NiSi, which is close to around 20% by lattice constant calculation,³² believed to be the strain limit. Moreover, the strain found in the Si region may not reflect all the strain energy since part of the strain energy may be absorbed by the

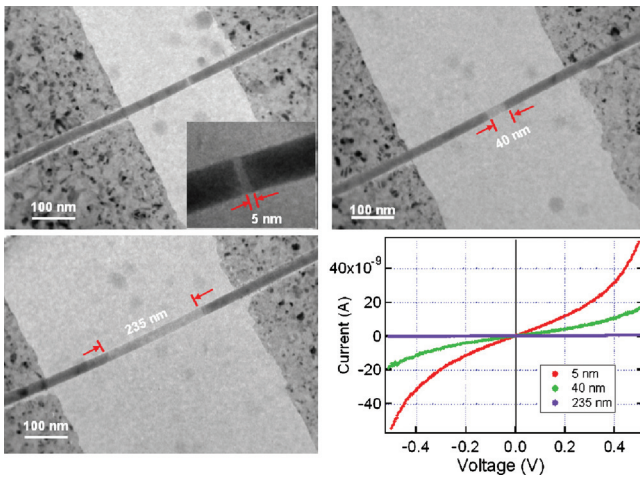


FIG. 4. (Color) Ni silicide/Si/Ni silicide devices of variable channel length from solid-state reactions and the corresponding transport measurements.

Si oxide. Therefore, the existence of this large strain is reasonable for the unique approach.

Figure 4 shows the electrical properties of the devices based on the Ni silicide/Si/Ni silicide nanoheterostructures, indicating that the current output increased as the Si channel length decreased and the compressively strain has risen. The current output is related to the channel length as shown below,

$$I \sim \frac{1}{R} = \frac{A}{\rho L},$$

ρ , A , and L are the conductivity, cross-sectional area, and channel length of the nanowires, respectively.³³ Theoretically, the current output should have increased eight times as the channel length shrank from 40 to 5 nm; however, practically, the current output increased only around twice since the compressively strain may have decreased the carrier mobility.

Understanding the fundamentals of nanowire growth is of great importance to optimize nanowire positioning. In the previous works, we can control the remaining length of the Si region between the two NiSi regions,²¹ and in turn, the strain of remaining Si can also be tuned with appropriate spacing. The properties of the nanostructure electronics are expected to be significantly impacted by the existent strain for potential applications of one-dimensional nanoheterostructures in nanoelectronic devices.

In conclusion, we have demonstrated that the NiSi/Si/NiSi nanoheterostructures contain highly strained Si by *in situ* TEM observation. Counting the number of (111) lattice planes in the Si region, we can determine the strain and we find that the Si is highly compressed. From the growth rate, we are able to control the formation of nanoheterostructures of silicide/Si/silicide down to a few nanometers or even atomic scale. Additionally, knowing the relationship between strain and spacing of the Si region, we can control the strain of the remaining Si. Furthermore, correlation among the current output, the Si channel length, and the compressive strain has been found in our electrical measurements on the nanodevices from such nanoheterostructures. We may tune the

current output by controlling the Si channel length and the compressive strain based on this study.

W.W.W. and K.C.L. acknowledge the support of the National Science Council through Grant Nos. 97-2218-E-009-027-MY3, 97-2120-M-009-006, 99-2120-M-007-011 and 98-2218-E-006-249, 99-2221-E-006-131. The first two authors contributed equally to this work.

¹X. Duan, Y. Huang, Y. Cui, J. Wang, and C. M. Lieber, *Nature (London)* **409**, 66 (2001).

²Y. Cui and C. M. Lieber, *Science* **291**, 851 (2001).

³Y. Huang, X. Duan, Y. Cui, L. J. Lauhon, K. Kim, and C. M. Lieber, *Science* **294**, 1313 (2001).

⁴Y. Xia, P. Yang, Y. Sun, Y. Wu, B. Mayers, B. Gates, Y. Yin, F. Kim, and H. Yan, *Adv. Mater. (Weinheim, Ger.)* **15**, 353 (2003).

⁵Y. Huang, X. Duan, Y. Cui, and C. M. Lieber, *Nano Lett.* **2**, 101 (2002).

⁶Y. Wu, J. Xiang, C. Yang, W. Lu, and C. M. Lieber, *Nature (London)* **430**, 61 (2004).

⁷W. M. Weber, L. Geelhaar, A. P. Graham, E. Unger, G. S. Duesberg, M. Liebau, W. Pamlar, C. Chèze, H. Riechert, P. Lugli, and F. Kreupl, *Nano Lett.* **6**, 2660 (2006).

⁸E. Lind, A. I. Persson, L. Samuelson, and L.-E. Wernersson, *Nano Lett.* **6**, 1842 (2006).

⁹M. Jeong, B. Doris, J. Kedzierski, K. Rim, and M. Yang, *Science* **306**, 2057 (2004).

¹⁰H. H. Liu, X. F. Duan, X. Y. Qi, Q. X. Xu, H. O. Li, and H. Qian, *Appl. Phys. Lett.* **88**, 263513 (2006).

¹¹L. Romano, A. M. Piro, M. G. Grimaldi, G. Bisognin, E. Napolitani, and D. D. Salvador, *Phys. Rev. Lett.* **97**, 136605 (2006).

¹²S. H. Olsen, A. G. O'Neill, P. Dobrosz, S. J. Bull, L. S. Driscoll, S. Chattopadhyay, and K. S. K. Kwa, *J. Appl. Phys.* **97**, 114504 (2005).

¹³C. N. Liao, K. C. Chen, W. W. Wu, and L. J. Chen, *Appl. Phys. Lett.* **87**, 141903 (2005).

¹⁴J. H. He, W. W. Wu, Y. L. Chueh, C. L. Hsin, L. J. Chen, and L. J. Chou, *Appl. Phys. Lett.* **87**, 223102 (2005).

¹⁵C. H. Liu, W. W. Wu, and L. J. Chen, *Appl. Phys. Lett.* **88**, 023117 (2006).

¹⁶C. H. Liu, W. W. Wu, and L. J. Chen, *Appl. Phys. Lett.* **88**, 133112 (2006).

¹⁷H. C. Hsu, W. W. Wu, H. F. Hsu, and L. J. Chen, *Nano Lett.* **7**, 885 (2007).

¹⁸Y. C. Chou, W. W. Wu, S. L. Cheng, B. Y. Yoo, N. V. Myung, L. J. Chen, and K. N. Tu, *Nano Lett.* **8**, 2194 (2008).

¹⁹Y. C. Chou, W. W. Wu, L. J. Chen, and K. N. Tu, *Nano Lett.* **9**, 2337 (2009).

²⁰K. C. Chen, W. W. Wu, C. N. Liao, L. J. Chen, and K. N. Tu, *Science* **321**, 1066 (2008).

²¹K. C. Lu, W. W. Wu, H. W. Wu, C. M. Tanner, J. P. Chang, L. J. Chen, and K. N. Tu, *Nano Lett.* **7**, 2389 (2007).

²²K. C. Lu, K. N. Tu, W. W. Wu, L. J. Chen, B. Y. Yoo, and N. V. Myung, *Appl. Phys. Lett.* **90**, 253111 (2007).

²³J. B. Hannon, S. Kodambaka, F. M. Ross, and R. M. Tromp, *Nature (London)* **440**, 69 (2006).

²⁴Y. Cui, L. J. Lauhon, M. S. Gudixsen, J. Wang, and C. M. Lieber, *Appl. Phys. Lett.* **78**, 2214 (2001).

²⁵R. S. Wagner and W. C. Ellis, *Appl. Phys. Lett.* **4**, 89 (1964).

²⁶S. Shingubara, O. Okino, Y. Sayama, H. Sakaue, and T. Takahagi, *Solid-State Electron.* **43**, 1143 (1999).

²⁷F. H. M. Spit, D. Gupta, and K. N. Tu, *Phys. Rev. B* **39**, 1255 (1989).

²⁸K. N. Tu, J. W. Mayer, and L. C. Feldman, *Electronic Thin Film Science* (Macmillan, New York, 1992).

²⁹S. S. Lau and M. A. Nicolet, in *Materials and Process Characterization*, edited by N. G. Einspruch and G. B. Larrabee (Academic, New York, 1983), p. 329.

³⁰K. L. Kavanah, *Semicond. Sci. Technol.* **25**, 1 (2010).

³¹G. Kästner and U. Gösele, *Philos. Mag.* **84**, 3803 (2004).

³²L. J. Chen, *Silicide Technology for Integrated Circuits* (The Institution of Engineering and Technology, London, 2004), p. 101.

³³S. M. Sze and K. K. Ng, *Physics of Semiconductor Devices* (Wiley, New York, 2007).